Brillouin-Enhanced Hyperparametric Generation of an Optical Frequency Comb in a Monolithic Highly Nonlinear Fiber Cavity Pumped by a cw Laser

Danielle Braje,* Leo Hollberg, and Scott Diddams

National Institute of Standards and Technology, 325 Broadway, Boulder, Colorado 80305, USA

(Received 18 September 2008; published 14 May 2009)

We demonstrate self-seeded generation of a broadband comb in a highly nonlinear fiber resonator. When pumped with a cw laser, the fiber cavity generates a comb with two characteristic spacings. Hyperparametric modes spaced by ~2 THz create the base structure of the comb, while commensurate Brillouin modes spaced by ~10 GHz populate the intermediate frequency gaps. The frequency modes are coherent, and the repetition rate of the comb has been locked to a microwave standard.

DOI: 10.1103/PhysRevLett.102.193902 PACS numbers: 42.65.Ky, 42.60.Da, 42.65.Es, 42.65.Yj

Introduction.—The ability to create a simple, coherent optical frequency comb has potential applications in precision measurement, short-pulse generation, microwave production, arbitrary optical and rf waveform engineering, and astronomy. In particular, generation of an optical comb with modes spaced by tens of gigahertz is especially useful because the resulting comb may be easily divided into its constituents for access and control of individual modes, and the coherent connection to radio frequencies enables low-phase-noise electronic signals. Historically, frequency combs were generated through electro-optic phase modulation of a laser [1,2] or by use of the output of a mode-locked laser where the net gain is higher for a train of short pulses than for cw operation. Recent interest, however, has centered on comb generation in compact monolithic resonators. The combination of small mode volume and high quality factors (Q) makes monolithic resonators with nonlinear gain an ideal medium for efficient nonlinear optical processes. Previous work on nonlinear optics in monolithic resonators focuses on whispering-gallery modes and includes generation of frequency combs in microtoroids [3], four-wave mixing in microspheres [4] and microrings [5], and coherent backscattering and oscillation in $LiNiO_3$ and CaF_2 gain-based resonators [6].

Here, we report a substantially different monolithic-resonator approach based upon a fiber, Fabry-Pérot (FP) cavity. In contrast to whispering-gallery resonators, which have multiple families of modes, FP resonators have a single well-defined cavity mode for a given input polarization. The macroscopic system is robust and easily coupled by free-space propagation or with standard telecom fibers, and the dispersion can be tailored via material and waveguide properties as well as with dielectric coatings. The trade-off is a lower Q value and larger mode volume, both of which increase the laser power necessary for nonlinear generation.

Our approach further differs from previous work by the multiplicative nature of the generated comb. Similar to the Raman combs of Harris [7] and Sokolov [8], which generate frequencies that are spaced near rotational and vibrational molecular resonances, the fiber-resonator comb has two characteristic spacings. Here, however, unrelated nonlinearities seed a coherent comb. First, ~2 THz spacing based on cascaded parametric generation originates from a modulation instability in the fiber and determines the overall spectral width at nearly 200 nm. Second, more narrowly spaced ~10 GHz modes build from stimulated Brillouin gain. In contrast to the molecular-based multiplicative spectrum, where the vibrational modes need not be an integer of the rotational frequency, the repetitive nature of the FP resonances forces the fiber-resonator comb to have a commensurate spectrum of modes when operated in a fundamental mode of the cavity.

Cavity design and nonlinearities.—The heart of the experiment is a monolithic cavity composed of a short section of dispersion-flattened fiber that has mirror-coated end faces. The commercially available fiber, which is called highly nonlinear fiber (HNLF) due to its comparatively small core, is made of a GeO_2-doped SiO_2 high delta core and depressed F-doped cladding. The mode field diameter is ~4 μm and dispersion slope at 1550 nm is less than 0.02 $ps/nm^2/km$ (33 fs^3/mm) [9]. Each fiber end

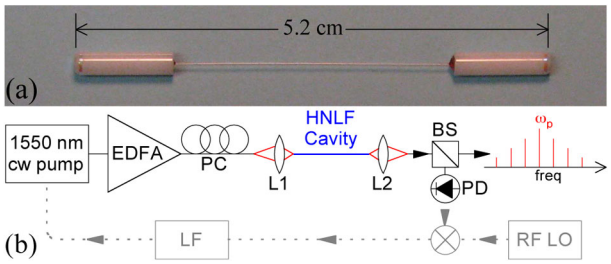

FIG. 1 (color online). (a) Photograph of a 5.2 cm-long highly nonlinear fiber (HNLF) cavity. Fiber ends are potted in ferrules, polished and mirror coated. (b) A cw laser traverses an erbium-doped fiber amplifier (EDFA) and a polarization controller (PC) before pumping the HNLF resonator. Lenses (L1 & L2) mode match between the telecom and HNLF fibers. The comb output from the cavity is divided by a beam splitter (BS); the light from one port is monitored on a high speed photodiode (PD). To lock the repetition rate of the comb, the detected beat note is mixed with an rf local oscillator (LO) and is fed back to the laser through a loop filter (LF).

is mounted in a standard ceramic ferrule for ease of handling, as can be seen in the photograph of Fig. 1(a). The end facets are polished and then coated with a dispersion-flattened dielectric coating, which has a peak reflectivity of 99.9% and is centered at 1550 nm. A scan of the transmitted optical power as a function of pump laser detuning over a cavity free spectral range (FSR) is shown in Fig. 2(a). The measured cavity finesse is >550. Because of stress-induced birefringence primarily resulting from fiber mounting, two closely spaced cavity modes are present [10]. Both polarization modes have a free spectral range of ~2 GHz, as determined by the length of the fiber [FSR = $c/(2n_gL)$, where c is the speed of light, n_g is the group index, and L is the fiber length]. The small frequency offset between the two polarization modes is on the order of a few hundred megahertz and varies from cavity to cavity. Either birefringent mode may be suppressed by adjusting the polarization of the pump laser. During comb generation, a single cavity mode is optimized, and the pump laser is locked on the side of the cavity resonance near the peak transmission. A thermal runaway effect as shown in Fig. 2(b) prohibits a cavity peak lock.

An additional advantage of the HNLF fiber-resonator comb lies in the simplicity of the experimental system, as can be seen in Fig. 1(b). An external-cavity diode laser (ECDL) is amplified by an erbium-doped fiber amplifier. The polarization of the cw laser is optimized to excite a single cavity mode, and light from the standard telecom fiber is mode matched into the smaller core of the HNLF. The generated comb may be analyzed in free space (preserving temporal profile) or efficiently coupled into telecom fiber. The comb properties are measured with a grating-based optical spectrum analyzer revealing the spectrum as a function of wavelength and with a fast photodetector to study the rf structure.

The cavity has gain at two characteristic frequencies that develop from disparate nonlinearities and that may be studied somewhat independently. A complete theoretical analysis of the interplay of all nonlinearities is quite involved, requiring a solution of a series of coupled nonlinear Schrödinger equations accounting for bidirectional propagation, periodic boundary conditions of the cavity as well as for material and waveguide contributions to phase-matching. Here, we focus on the predominant nonlinearities. The widely spaced modes, which result from hyperparametric processes, are shown in Fig. 3(a). In this plot, stimulated Brillouin scattering (SBS) has been suppressed by modulating the pump laser at a frequency that is not a divisor of the Brillouin shift. Previous studies on the shape of the gain curve in nonlinear fibers and fiber cavities [11] predict the location of the nearest modes. The first signal and idler modes are created through nondegenerate four-wave mixing, the position of which is determined through phasematching as well as by the zero dispersion point in the fiber. The four-wave mixing process is referred to as a modulation instability in fiber optics [12]. Although initially seen only in the anomalous dispersion regime of fibers, the use of a dispersive cavity can expand the realm of modulation instability into the range of normal dispersion [13], where Raman gain can be suppressed. Through a series of cascaded four-wave mixing (or hyperparametric) processes, the remaining 2 THz modes are created with the expected triangular shape as a function of optical frequency. From the perspective of quantum mechanics, this is interesting due to the entangled nature of the generated photons [14].

The second characteristic frequency spacing populates the space between the hyperparametric modes. When the

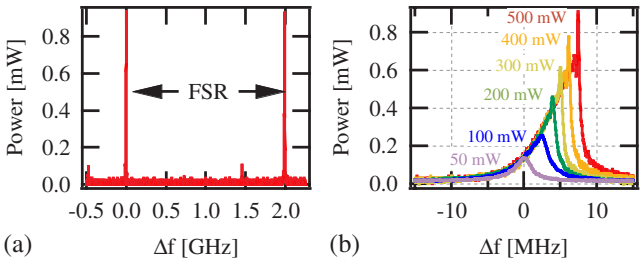

FIG. 2 (color online). (a) The laser is tuned across a cavity FSR. Slight polarization rotation reveals the birefringent mode shifted by ~500 MHz. (b) Thermal runaway as the pump laser is tuned through cavity resonance.

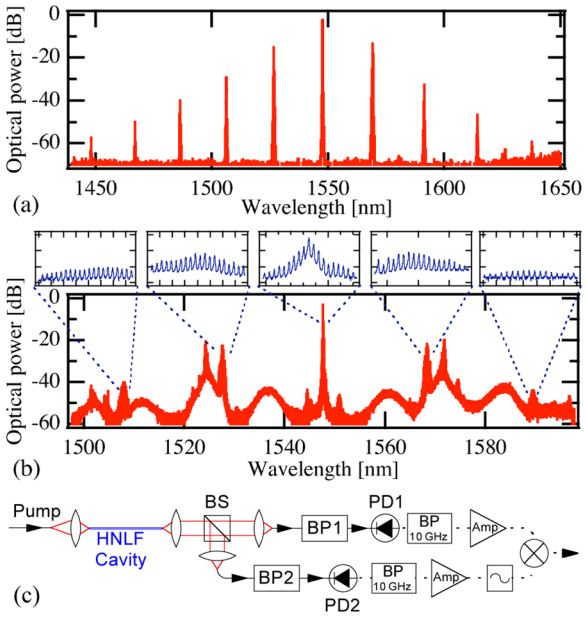

FIG. 3 (color online). (a) Hyperparametric modes of the HNLF fiber when pumped with 550 mW near 1550 nm. To suppress SBS, the pump laser is externally modulated at 8 GHz. (b) Stimulated Brillouin modes with spacing of 9.87 GHz populate the intermediate frequency band between the terahertz modes. Each inset depicts a 1.5 nm wide region with the same vertical scale to reveal the individual modes across the spectrum. (c) Schematic of coherence measurement. Optical bandpass filters (BP1 & BP2) select different optical spectral regions that are detected on high speed photodiodes (PD1 & PD2). The rf signals are filtered and amplified before the mixer (⊗). A phase shifter (~) adjusts the relative delay in optical and electrical paths.

parametric modes reach the SBS threshold, the Brillouin gain near 10 GHz dominates, and uniform modes across the spectrum are self-generated, as seen in Fig. 3(b). An assemblage of 1.5 nm wide insets shows the individual 10 GHz modes across different spectral regions. Stimulated Brillouin scattering, or scattering of light by longitudinal optical phonons, produces a Stokes beam that is counterpropagating to the pump laser. The frequency shift $\Delta\nu_B$ of the Stokes beam is determined primarily by the bulk properties of the material [$\Delta\nu_B = 2n(\lambda)v_s/\lambda$, where $n(\lambda)$ is the index of refraction, v_s is the sound velocity in the material, and λ is the wavelength of the pump laser]. Because of the periodic boundary conditions of the cavity, there is an additional frequency pulling effect that forces the gain peak to be an integral number of cavity modes. Although SBS is best known for its parasitic nonlinearity, which typically limits power in optical fibers, ideal features such as relative line narrowing have increased interest throughout the last decade [15,16]. The cavity further enhances the linewidth narrowing effect as $\Delta\nu_S = \Delta\nu_p(1 + \pi\gamma/\Gamma)^{-2}$ where the optical linewidth $\Delta\nu_S$ of the Stokes frequency is reduced from that of the pump $\Delta\nu_p$ as governed by the Brillouin gain bandwidth γ and the optical loss of the cavity Γ [15]. For a measured $\gamma = 79$ MHz, linewidth narrowing on the order of 4×10^3 may be possible. Brillouin lasers are built upon this principle by output coupling the narrowed counterpropagating Brillouin mode [17]. The relative linewidth narrowing of the Brillouin modes with respect to the input laser enables generation of microwave signals with lower phase noise [18].

Although phasematching forces the generated SBS frequency to counterpropagate with respect to the pump laser, the cavity nature of resonator promotes bidirectional propagation. This gives rise to cascaded SBS, where each Stokes wave acts as a pump for successive Stokes waves [15]. Once the Brillouin frequency modulation is established, cross-phase modulation ensures that additional sidebands have a uniform frequency shift. If the system oscillated solely on Brillouin gain, the generated modes would have a wavelength-dependent frequency shift due to the change in index as a function of wavelength. At $\lambda \approx 1550$ nm, a shift of $\Delta\nu_B$ of -6.4 MHz/nm was measured in a 50 m long HNLF.

Coherence measurement.—To test the self-coherence of the spectrum and ensure that the intermediate modes have a constant frequency spacing, 10 GHz modes from different spectral regions are compared. The microwave setup is shown in Fig. 3(c). After the HNLF resonator, a nonpolarizing beam splitter divides the comb before the light couples into single-mode fibers. In each arm, 2 nm wide optical bandpass filters centered at 1533 and at 1567 nm select different spectral components, and the two wavelength regions are detected by high speed photodiodes. Microwave filters pass the 10 GHz rf spectra, and the signals are amplified to +7 dBm for the local oscillator and to +1 dBm for the rf signal before the mixer. A phase shifter in the rf arm is adjusted to account for the relative delay in optical and electrical path lengths. The baseband output of the mixer compares the 10 GHz beatnotes from each portion of the spectrum. When the Brillouin gain is not large enough to completely populate the region between the parametric modes, each group of comb modes has an independent repetition rate, and the baseband output of the mixer has a sinusoidal output. However, when the resonator is operating with a continuous spectrum, such as that of Fig. 3(b), the output of the mixer is a dc signal with rms phase noise <3 mrad in one second, verifying that different portions of the spectrum have the same frequency-mode spacing when a continuous comb is produced. Because both optical paths are required for this experiment, the pump laser is free running without a sidelock to the cavity mode. Nonetheless, the system maintains a coherent dc mixed signal for over 30 minutes, demonstrating that the relative microwave phase is stable over time.

Repetition rate locking.—In addition to showing optical coherence, the 10 GHz beat frequency can be locked to an external oscillator, as shown in Fig. 1(b), and the repetition rate may be tuned by a few hundred kilohertz without unlocking. The method for tuning the repetition rate stems from the dependence of the Brillouin frequency on the wavelength of the pump laser, with a further enhancement in tuning range as a result of the thermal runaway ramp caused by a length expansion and a thermo-optic effect in index of refraction. As the laser is tuned up the ramp, the corresponding change in $\Delta\nu_B$ enables tuning of the repetition rate. An error signal is created by detecting a portion of the comb on a high speed photodetector and mixing the signal with a reference oscillator. The error signal is fed back to the piezoelectric transducer or the current feedback of the ECDL in order to tune and lock the repetition rate. Scanning the pump laser across many cavity FSR enables a larger tuning range. Although frequency pulling is possible by adjusting the length of the cavity, the overall cavity length (or an integral number of cavity lengths) must fall under the Brillouin gain peak. If a further jump in $\Delta\nu_B$ is required, cavity fabrication may be tailored to specific design parameters. For example, adjusting the GeO_2 content of the fiber core changes the velocity of sound in the medium and shifts the Brillouin frequency [19].

Pump power dependence.—Figure 4 shows the evolution of the optical spectrum as a function of laser power. At a pump power of 500 mW in Fig. 4(a), only the hyperparametric modes can be seen. Without intensity modulation, however, a small number of SBS modes are present on each of the 2 THz peaks. Note that when the Brillouin shift is not in a fundamental cavity mode or the gain is not high enough to continuously fill the large gaps, the Brillouin modes need not be commensurate at different spectral regions. As the power is increased to 520 mW in Fig. 4(b), an intermediate peak develops at 1 THz spacing. In Figs. 4(c) and 4(d), midspectral regions are populated by the self-seeded Brillouin modes and cross-phase modulation. It should be noted that once the HNLF cavity is Brillouin

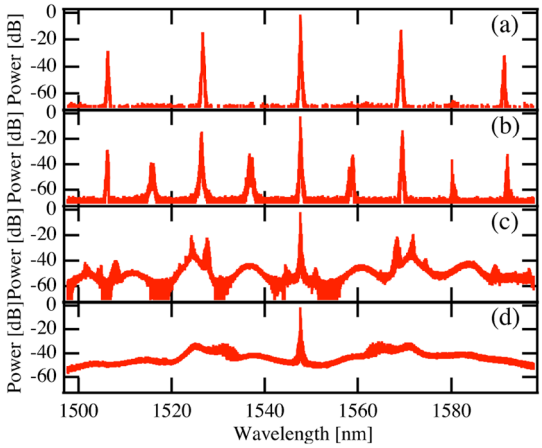

FIG. 4 (color online). Output of the HNLF cavity with pump powers of (a) 500, (b) 520, (c) 540, and (d) 560 mW.

"lasing," a hysteretic effect in pump power is evident; the pump power may be decreased without loss of modes. As a result of the 2 GHz resolution limit of the optical spectrum analyzer, close inspection of Fig. 4(d) appears to depict a continuous spectrum, as opposed to individual modes. Because the Brillouin frequency is not the fundamental frequency of the cavity, but rather 5 FSR, 2 GHz modes fill in the intermediate regions and cannot be resolved. We are in the process of fabricating shorter cavities, which should eliminate the additional modes.

In the described experiments, the 10-GHz comb modes have *self-generated* through SBS. Instead, the narrowly spaced modes can be *seeded* at an integral number of cavity FSR. In the spirit of a dual-pumped optical parametric oscillator [20], an intensity-modulated pump drives the resonator; nonlinear generation has been observed at integer numbers up to 10 FSR with spectral widths of 100 nm. Brillouin modes may be suppressed by choosing the cavity length such that integers of FSR are detuned from the Brillouin gain peak.

Conclusion.—We have studied experimentally a new type of monolithic comb resonator that lases with a multiplicative spectrum of widely spaced as well as narrow commensurate modes. The spectral width of the comb exceeds 150 nm, and the comb modes are shown to be mutually coherent. Adjusting the frequency of the pump laser controls the comb repetition rate and enables locking to a microwave standard. Achieving relatively narrow-linewidth modes, such as those from Brillouin lasing, allows for the creation of compact, narrow-linewidth sources and frequency converters. In addition, the properties of monolithic fiber combs such as cavity Q, length, and dispersion are readily tailorable. Combs derived from SBS are interesting for low-noise microwave generation, spectroscopic studies, or coherent tomography, and the parametric modes could prove useful in the production of nonclassical states of light.

The authors gratefully acknowledge J. Hall, T. Kippenberg, P. Del'Haye, and R. Holzwarth for discussions in the preliminary stages. We thank S. Dyer for the long HNLF and B. Swann for the ECDL. This work is a contribution of NIST, an agency of the US government, and is not subject to copyright.

*braje@stanfordalumni.org

[1] T. Kobayashi *et al.*, Appl. Phys. Lett. **21**, 341 (1972); M. Kourogi, K. Nakagawa, and M. Ohtsu, IEEE J. Quantum Electron. **29**, 2693 (1993); L. R. Brothers, D. Lee, and N. C. Wong, Opt. Lett. **19**, 245 (1994).
[2] A. S. Bell, G. M. Mcfarlane, E. Riis, and A. I. Ferguson, Opt. Lett. **20**, 1435 (1995); S. Diddams, L.-S. Ma, J. Ye, and J. L. Hall, Opt. Lett. **24**, 1747 (1999).
[3] T. J. Kippenberg, S. M. Spillane, and K. J. Vahala, Phys. Rev. Lett. **93**, 083904 (2004); P. Del'Haye *et al.*, Nature (London) **450**, 1214 (2007).
[4] I. H. Agha, Y. Okawachi, M. A. Foster, J. E. Sharping, and A. L. Gaeta, Phys. Rev. A **76**, 043837 (2007).
[5] A. C. Turner, M. A. Foster, A. L. Gaeta, and M. Lipson, Opt. Express **16**, 4881 (2008).
[6] A. A. Savchenkov *et al.*, Phys. Rev. Lett. **93**, 243905 (2004); M. Mohageg, A. Savchenkov, and L. Maleki, Opt. Lett. **32**, 2574 (2007); A. A. Savchenkov *et al.*, Phys. Rev. Lett. **101**, 093902 (2008).
[7] D. D. Yavuz, D. R. Walker, M. Y. Shverdin, G. Y. Yin, and S. E. Harris, Phys. Rev. Lett. **91**, 233602 (2003).
[8] A. M. Burzo, A. V. Chugreev, and A. V. Sokolov, Phys. Rev. A) **75**, 022515 (2007).
[9] J. Kubo *et al.*, in *Proc. 16th Eur. Conf. Opt. Commun., Amsterdam, 1990* (IOS, Amsterdam, 2008), p. 505; C. Joergensen *et al.*, in *Proc. 29th Eur. Conf. Opt. Commun., Rimini, 2003* (Assoc. Elettrotec. Elettron. Ital., Milan, 2003).
[10] M. Tateda, K. Komaki, and Y. Yamaguchi, Electronics and Communications in Japan **90**, 1 (2007).
[11] M. E. Marhic, N. Kagi, T.-K. Chiang, and L. G. Kazovsky, Opt. Lett. **21**, 573 (1996); M. Yu, C. J. McKinstrie, and G. P. Agrawal, J. Opt. Soc. Am. B **15**, 617 (1998).
[12] G. Agrawal, *Nonlinear Fiber Optics* (Elsevier, New York, 2007), 4th ed., Chap. 5.
[13] M. Haelterman, S. Trillo, and S. Wabnitz, Opt. Commun. **91**, 401 (1992).
[14] J. Chen, X. Li, and P. Kumar, Phys. Rev. A **72**, 033801 (2005).
[15] A. Debut, S. Randoux, and J. Zemmouri, Phys. Rev. A **62**, 023803 (2000).
[16] I. S. Grudinin, A. B. Matsko, and L. Maleki, arXiv:0805.0803.
[17] J. Geng, S. Staines, Z. Wang, J. Zong, M. Blake, and S. Jiang, IEEE Photonics Technol. Lett. **18**, 1813 (2006).
[18] S. Norcia, S. Tonda-Goldstein, D. Dolfi, J.-P. Huignard, and R. Frey, Opt. Lett. **28**, 1888 (2003).
[19] R. Tkach, A. Chraplyvy, and R. Derosier, Electron. Lett. **22**, 1011 (1986).
[20] S. Radic and C. McKinstrie, IEICE Trans. Electron. **E88-C**, 859 (2005).